

# Experimental Results for 25-mm and 51-mm RDRE Combustors

Carl Knowlen, Tyler Mundt, and Mitsuru Kurosaka  
William E. Boeing Department of Aeronautics and Astronautics, University of Washington  
Seattle, WA 98195, USA

## 1 Introduction

Understanding the physics that limit the smallest size scale at which spinning detonation waves can exist will allow appropriate integration of miniaturized RDRE technology with advanced propulsion system concepts to reduce system mass and complexity while also potentially enhancing performance. The objective of the ongoing research program at the University of Washington is to determine the influence of combustor radius of curvature on the operating characteristics of the RDRE in a systematic manner. Toward this end, three geometrically similar RDRE test rigs have been designed, fabricated and tested with combustor annulus diameters of 75-mm, 51-mm, and 25-mm. The gap width of 5-mm was kept the same in all designs. Presented here are the results of recent 51-mm-RDRE and 25-mm-RDRE experiments with flat-faced, impinging injectors utilizing methane-oxygen propellant.

## 2 Experimental Facility

The High Enthalpy Flow Laboratory at the University of Washington is located in an interior laboratory space of the Aerospace Energetics Research Building. This facility has a 4 m<sup>3</sup> dump tank rated to 0.7 MPa working pressure with 500 kg of aluminum alloy plates for capturing and condensing combustion effluent. Connecting the dump tank to the RDRE test rig is a series of pipe sections and a 0.25-m wye tube, which routes the combustion effluent to the dump tank while allowing optical access to the RDRE combustion chamber, as shown in Fig. 1. The wave dynamics within the RDRE combustors are observed at 240,000 FPS with a Phantom v12.11 camera using a 70-200 mm zoom lens. The oxidizer and fuel flow control systems utilize electronic regulators and factory calibrated critical nozzles to control and meter flow. This system can fuel the test rigs at propellant flow rates up to 0.5 kg/s for run durations of up to 2 seconds without raising the dump tank pressure more than 30 kPa. Pressure transducers (Omega PX319-500) are mounted at the end of standoff tubes having an internal passage length-to-diameter ratio of 145 and are sampled at 2 kHz via a National Instruments-based 64-channel data acquisition system. These sensors provide axial pressure profiles in the annulus. A sparkplug-ignited pre-detonator at the exit of the RDRE initiates detonation in the combustor annulus.

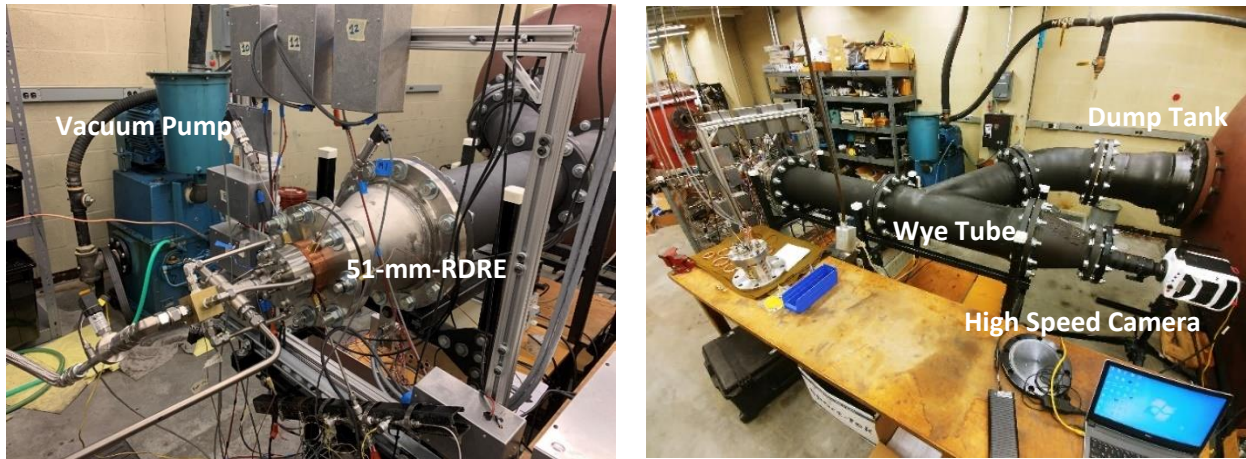


Figure 1 High enthalpy test facility. Left: 51-mm-RDRE rig installed on test stand. Right: Wye tube routes effluent to dump tank to enable direct view of combustor with the high-speed camera.

### 3 RDRE Geometry

Geometrically scaled RDREs with constant annulus gap of 5 mm were designed and fabricated with annulus outer diameters of 25.4 mm and 50.8 mm (Fig. 2). The corresponding inner core diameters were 15.4 mm and 40.8 mm, respectively, with lengths equal to their annulus OD. The inner and outer walls were fabricated from OFHC copper and the flat-faced impinging injectors were brass. Modular design allows cores to be swapped out to adjust annular gap and inner core length. The 51-mm-RDRE had 3 sidewall ports. The sparkplug port near the middle of annulus was used for the pre-detonator. The 25-mm-RDRE had 4 sidewall instrument ports plus one at the exit for the pre-detonator.

The oxidizer-to-fuel injector port area ratio (2.50) was sized to ideally have similar plenum pressure levels when operating at near stoichiometry conditions for  $\text{CH}_4/\text{O}_2$  propellant. The injector orifices were scaled to have same injector-to-gap area ratio,  $\text{AR} = 0.11$ , (i.e., net injector throat area to gap area) for a 5-mm-gap at each combustor annulus OD. The 51-mm-RDRE injector had 72 port-pairs and the 25-mm-RDRE injector had 48 port-pairs with the azimuthal center-to-center spacing (Center  $\Delta$ ) between injectors reduced proportionally to the reduction in OD and radial spacing kept constant at 2.34 mm. Injectors and their section views are shown in Fig. 3. Injector details are listed in Table 1. Each injector ring was inclined  $30^\circ$  to the axis resulting in an impingement height of 2.16 mm.

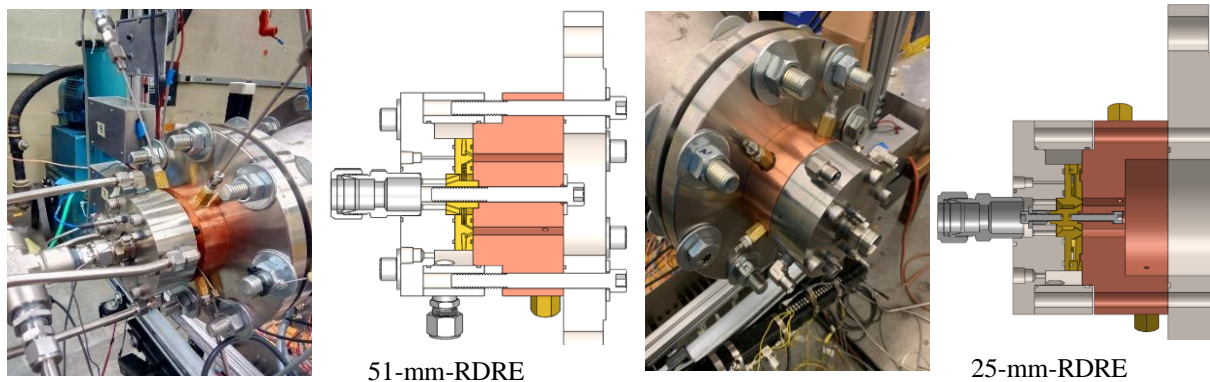


Figure 2 51-mm and 25-mm RDRE configurations. Outer plenum for  $\text{O}_2$ , inner plenum for fuel.

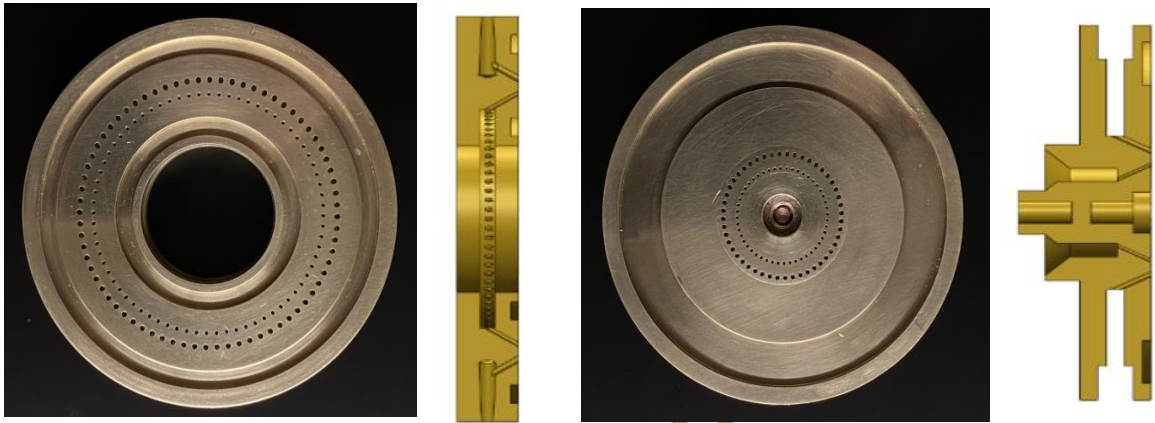


Figure 3 Flat-faced, impinging injectors. Left: 51-mm-RDRE. Right: 25-mm-RDRE injector.

Table 1 Injector parameters

Injector	Fuel Port Dia, mm	Ox Port Dia, mm	Injector Pairs	Fuel Center $\Delta$ , mm	Ox Center $\Delta$ , mm	Radial Center $\Delta$ , mm
51A-5	0.64	0.99	72	1.89	2.09	2.34
25A-5	0.51	0.81	48	1.18	1.46	2.34

## 4 Experimental Procedure

Experiments with different RDRE combustors having a factor of two difference in radius of curvature and the same 5-mm-gap were carried out while keeping the ranges of mass flux and equivalent ratio of  $\text{CH}_4/\text{O}_2$  propellant constant. This enabled results to be compared at the same injection pressure and propellant density, and thus same detonation cell size [1]. These experiments with flat-faced impinging injectors utilized  $\text{AR} = 0.11$  in all cases to eliminate potential wave dynamic differences in the combustor due to plenum back-pressurization effects [2]. The dump tank and test rig were evacuated to around 50 kPa prior to each experiment. In all cases, the results were backpressure insensitive and were operated at sub-atmospheric exit conditions to allow the exhaust duct and dump tank to collect unburned propellant without any chance of it leaking into the lab. Backpressure sweeps were carried out to determine under what conditions the results are sensitive to exhaust pressure, which typically manifest themselves as reduced axial pressure gradient in the annulus and increased minimum mass flux for stable RDRE operation [3].

## 5 Experimental Results

The wave dynamics of combustors having different radii of curvature and injector configurations were compared for the same ranges of mass flux and equivalent ratio. Mass flux sweeps ranging from  $80 \text{ kg/s/m}^2$  to  $500 \text{ kg/s/m}^2$  were carried out at constant equivalence ratio of  $\phi = 1.15$ . Sweeps of equivalence ratio over  $0.25 < \phi < 2.5$  were carried out at constant mass flux of  $243 \text{ kg/s/m}^2$ . All data points represent the average of at least two experiments that were within 2% of the desired test conditions. Wave speeds were determined from the high-speed video in manner similar to that described in [4].

The mass flow rate vs. mass flux data in Fig. 4-left have plotting symbols that indicate the character of the wave dynamics observed at each test condition. Data from sweeps of  $\phi$  at constant mass flux are shown in Fig. 4-right. The open plotting symbols indicate RDRE operation without counter-rotating waves (CW). The lightly shaded plotting symbols have dominate rotating detonations of wave number  $n = 1$  with a single CW present. Deflagration without any indication of rotating waves is indicated by solid plotting symbols. No combustion occurred under the most fuel rich conditions in the 25A-5 configuration. Data at mass fluxes and equivalence ratios to be used for subsequent CFD modeling (not discussed here) are those along vertical dashed lines.

Mode transition in the 51-mm-RDRE is indicated in Fig. 4-left by a change in wave number from  $n = 2$  to  $n = 1$  when the mass flux was decreased from  $324 \text{ kg/s/m}^2$  to  $243 \text{ kg/s/m}^2$ . The wave speed increased 17% in this case. This result is consistent with the expectation that the detonation waves will adjust in speed and number to attain a balance in rates of propellant injection and product exhaust when stable operation is feasible. This same mass flux reduction also resulted in a mode transition in the 25-mm-RDRE, however, in this case operation went from  $n = 1$  to a condition where a CW appears with a dominate  $n = 1$  wave. This resulted in an 11% reduction in rotational frequency from 21 kHz to 19 kHz. The reduction in wave speed and lower combustor pressure seen when a CW is present may be a consequence of the cell size approaching a critical size limit for low flux and off stoichiometric test conditions [5]. Further reduction in mass flux led to deflagration, which is associated with lowest combustor pressure and thus the largest cell size for this test sequence.

Data plotted in Fig. 4-right show that the range of  $\phi$  on the fuel-lean and fuel-rich side of the stoichiometric region for mode transition increased as RDRE size scale decreased. In the 51-mm-RDRE,  $n = 1$  wave operation occurred in the  $1.0 < \phi < 1.2$  range and  $n = 2$  when outside of it. Whereas in the 25-mm-RDRE,  $n = 1$  wave operation with a CW occurred in the  $1.1 < \phi < 1.4$  range and  $n = 1$  without CW when outside of it. The lowest wave number in the 51-mm-RDRE was found to be at near stoichiometric conditions and the wave number increased by one when the propellant was made either more fuel lean or rich. Stable operation was observed at  $\phi \sim 1.8$  with  $n = 1$  and  $n = 2$  in the 25-mm and 51-mm RDREs, respectively. Deflagration with two weak waves occurred at  $\phi \sim 2.0$  in the 25-mm-RDRE and deflagration at  $\phi \sim 2.5$  was observed in both RDREs.

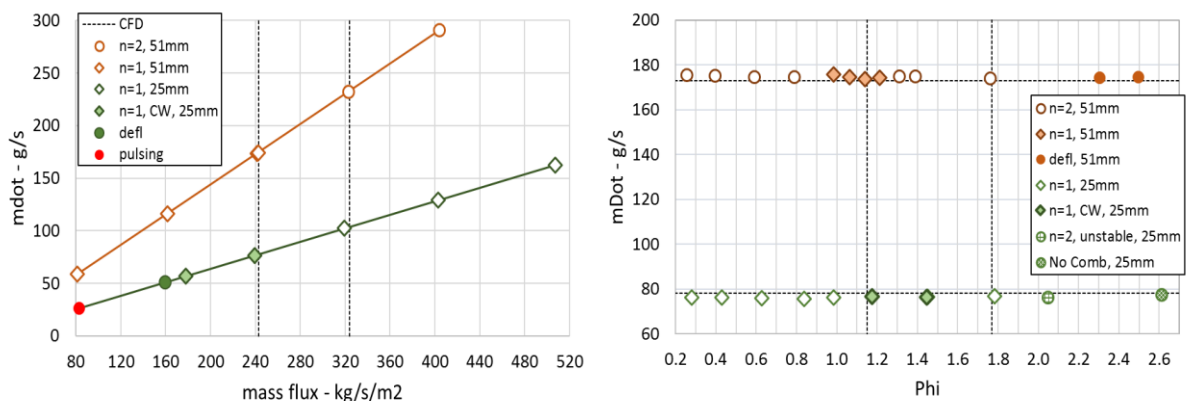


Figure 4 Mass flow rate data from 25-mm and 51-mm RDREs with 5-mm-gap,  $n =$  wave number. Left: Mass flux sweep at constant  $\phi = 1.15$ . Right:  $\phi$  sweep at constant mass flux =  $243 \text{ kg/s/m}^2$ .

The peripheral transverse wave spin speed as function of mass flux and equivalence ratio data for the 25-mm and 51-mm-RDREs are shown in Fig. 5. As mass flux increased at constant  $\phi = 1.15$  up to  $243 \text{ kg/s/m}^2$ , the wave spin speed increased in both RDREs (Fig. 5-left). When mass flux increased to  $324 \text{ kg/s/m}^2$  in the 51-mm-RDRE, however, the wave number increased from  $n = 1$  to  $n = 2$  and the corresponding spin speed decreased from  $2 \text{ km/s}$  to  $1.7 \text{ km/s}$ . In the 25-mm-RDRE, counter-rotating waves were present with a dominate  $n = 1$  wave when the mass flux was at and below  $243 \text{ kg/s/m}^2$ ,

Distribution Statement A: Approved for Public Release; Distribution is Unlimited. PA Clearance #AFRL-2021-2660.

whereas only a single  $n = 1$  wave occurred at  $324 \text{ kg/s/m}^2$  and above. The corresponding wave speed increased from  $1.55 \text{ km/s}$  to  $1.75 \text{ km/s}$  when the CWs disappeared. This change in wave dynamics is another kind of mode transition, which occurs at the same mass flux range in both RDREs under conditions where the propellant has the same cell size.

The periphery wave spin speed vs.  $\phi$  data are shown in Fig. 5-right. In the range  $0.25 < \phi < 0.8$ , both RDREs operated at the same wave spin speed with  $n = 1$  and  $n = 2$  for the 25-mm and the 51-mm annulus outer diameters, respectively. There was a relative maximum of  $1.7 \text{ km/s}$  at  $\phi = 0.6$  in both cases. The spin speed decreased with  $n = 1$  as  $\phi$  increased from  $0.8$  to  $1.0$  in the 25-mm-RDRE, and then a CW appeared in range  $1.15 < \phi < 1.4$  that further reduced the spin speed. The CW disappeared at  $\phi \sim 1.8$  and the spin speed increased from  $1.4 \text{ km/s}$  to  $1.5 \text{ km/s}$ . A distinct mode transition from  $n = 2$  to  $n = 1$  was observed in the 51-mm-RDRE when  $\phi$  increased from  $0.8$  to  $1.0$ , which is indicated by an increase in spin speed from  $1.65 \text{ km/s}$  to  $2 \text{ km/s}$ . At fuel-rich conditions with  $\phi \geq 1.3$ ,  $n = 2$  operation was re-established and the spin speed decreased accordingly. At  $\phi = 1.8$ , both RDREs operated at the same spin speed ( $\sim 1.5 \text{ km/s}$ ) even though they had different wave numbers.

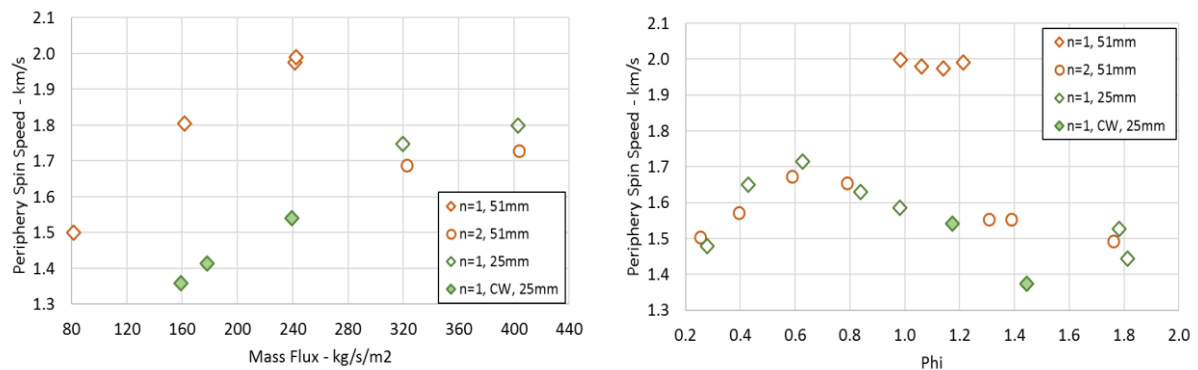


Figure 5 Spin speed data from 25-mm- and 51-mm-RDREs,  $n =$  wave number. Left: Mass flux sweep at constant  $\phi = 1.15$ . Right:  $\phi$  sweep at constant mass flux =  $243 \text{ kg/s/m}^2$ .

## 6 Conclusion

The wave dynamics in the annular combustors of 25-mm and 51-mm RDREs with 5-mm-gap were investigated over relatively wide ranges of mass flux ( $80 \text{ kg/s/m}^2$  to  $500 \text{ kg/s/m}^2$ ) and equivalence ratio ( $0.25 < \phi < 2.5$ ). The influence of flat-faced impinging injectors scaled to have the same net throat area-to-gap area ratio of  $AR = 0.11$  and impingement properties were examined. The spin frequency, peripheral spin speed, and number of waves were determined from high speed video of the annulus. Stable operation was established near stoichiometric conditions in both RDREs. At the extreme ends of the  $\phi$  range, however, counter-rotating waves, deflagration, and pulsing phenomena were observed. The nature of these features for a given propellant flow condition strongly depended on the annulus outer diameter. Mode transitions between  $243 \text{ kg/s/m}^2$  and  $324 \text{ kg/s/m}^2$  were seen in the mass flux sweeps at constant  $\phi = 1.15$  for annulus outer diameters of 25-mm and 51-mm. The influence of heat transfer in these small scale RDREs is still under investigation.

## Acknowledgments

Experiment assistance was greatly appreciated by Mark Ikeda, David Menn, Dani Nankova, Noah Takumi, Tharun Sanker and Lien Chang. Consultations with Bill Hargus and John Bennewitz were very helpful. This work was supported by AFOSR Grant FA 9550-18-1-9-0076 and the Office of Naval Research funding document N0001417MP00398.

## References

- [1] Schumaker SA, Knisely AM, Hoke JL, Rein KD. (2021). Methane–oxygen detonation characteristics at elevated pre-detonation pressures. *Proceedings of the Combustion Institute*. 38: 3623.
- [2] Koch JV, Chang L, Upadhye C, Chau K, Kurosaka M, Knowlen C. (2019). Influence of Injector-to-Annulus Area Ratio on Rotating Detonation Engine Operability. doi: 10.2514/6.2019-4038.
- [3] Koch JV, Washington MR, Kurosaka M, Knowlen C. (2019). Operating Characteristics of a CH<sub>4</sub>/O<sub>2</sub> Rotating Detonation Engine in a Backpressure Controlled Facility. doi: 10.2514/6.2019-0475.
- [4] Bennewitz JW, Bigler BR, Hargus WA, Danczyk SA, Smith RD. (2018). Characterization of Detonation Wave Propagation in a Rotating Detonation Rocket Engine using Direct High-Speed Imaging. doi:10.2514/6.2018-4688.
- [5] Bykovskii FA, Zhdan SA, Vedermikov EF. (2006). Continuous Spin Detonations. *AIAA Journal of Propulsion and Power*. 22: 1204.